Cysteine-scanning mutagenesis reveals a highly amphipathic, pore-lining membrane-spanning helix in the glutamate transporter GltT

Slotboom, DJ; Konings, WN; Lolkema, JS

Published in:
The Journal of Biological Chemistry

DOI:
10.1074/jbc.M011064200

Publication date:
2001

THE JOURNAL OF BIOLOGICAL CHEMISTRY
Vol. 276, No. 14, Issue of April 6, pp. 10775–10781, 2001
Printed in U.S.A.

Cysteine-scanning Mutagenesis Reveals a Highly Amphipathic, Pore-lining Membrane-spanning Helix in the Glutamate Transporter GltT*

Received for publication, December 8, 2000, and in revised form, January 5, 2001
Published, JBC Papers in Press, January 8, 2001, DOI 10.1074/jbc.M011064200

Dirk Jan Slotboom, Wil N. Konings, and Juke S. Lolkema‡

From the Department of Microbiology, Groningen Biomolecular Sciences and Biotechnology Institute, University of Groningen, 9751 NN Haren, The Netherlands

The carboxyl-terminal membrane-spanning segment 8 of the glutamate transporter GltT of *Bacillus stearothermophilus* was studied by cysteine-scanning mutagenesis. 21 single cysteine mutants were constructed in a stretch ranging from Gly-374 to Gln-404. Two mutants were not expressed, four were inactive, and two showed severely reduced glutamate transport activity. Cysteine mutations at the other positions were well tolerated. Only the two most amino- and carboxyl-terminal mutants (G374C, I375C, S399C, and Q404C) could be labeled with the large thiol reagent fluorescein maleimide, indicating unrestricted access and a location in a loop structure outside the membrane. The labeling pattern of these mutants using membrane- permeable and -impermeable thiol reagents showed that the N and C termini of the mutated stretch are located extra- and intracellularly, respectively. Thus, the location of the membrane-spanning segment was confined to a stretch of 23 residues between Gly-374 and Ser-399. Cysteine residues in three mutants in the central part of the segment (M381C, V388C, and N391C) could be labeled with the small and flexible reagent 2-aminoethyl methanethiosulfonate hydrobromide only, suggesting accessibility via a narrow aqueous pore. When the region was modeled as an α-helix, all positions at which cysteine mutations lead to inactive or severely impaired transporters cluster on one face of this helix. The inactive mutants showed neither proton motive force-driven uptake activity nor exchange activity nor glutamate binding. The results indicate that transmembrane segment 8 forms an amphipathic α-helix. The hydrophilic face of the helix lines an aqueous pore and contains many residues that are important for activity.

Glutamate transporters in the mammalian central nervous system remove the neurotransmitter glutamate from the synaptic cleft into surrounding neurons and glial cells. Removal of glutamate prevents neurotoxicity of high concentrations of glutamate and helps to end the excitatory signal at some synapses (1–4). The proteins are secondary transporters that couple glutamate transport against the concentration gradient to the transport of protons, sodium ions, and potassium ions across the membrane. The glutamate transporters belong to a large family of transport proteins in which are also found bacterial glutamate transporters including GltT of *Bacillus stearothermophilus* (5). Computational analyses of the amino acid sequences and hydropathy profiles of the glutamate transporters showed that the proteins form a unique structural class of membrane proteins, which is structurally not related to any other family of secondary transporters (5, 6). Subsequent experimental studies confirmed that the proteins contain unique structural features, like water-filled pores and pore loops, which are not found in "regular" secondary transporters (7–11).

The amino-terminal half of the transporters contains six membrane-spanning α-helices, with the amino terminus of the proteins located in the cytoplasm. The membrane topology of the carboxyl-terminal half of the transporters is still somewhat controversial. However, in the most generally accepted model the six amino-terminal α-helices are followed by a reentrant loop entering the membrane from the cytoplasmic side, a seventh membrane-spanning helix, a reentrant loop entering the membrane from the extracellular side and, finally, an eighth membrane-spanning segment, leaving the carboxyl terminus in the cytoplasm (Fig. 1). The eukaryotic and prokaryotic glutamate transporters differ predominantly in the length of their hydrophilic regions. Three hydrophilic stretches are considerably longer in the eukaryotic proteins: the amino-terminal and carboxyl-terminal extensions and the region between the third and fourth membrane-spanning segment, which is glycosylated in the eukaryotic members. Evidence is accumulating that the carboxyl-terminal half of the transporters, which is particularly well conserved, constitutes a major part of the translocation pathway and contains the binding sites for the substrate and cotransported ions (7, 12–18). The bacterial and eukaryotic glutamate transporters have different coupling ion specificity. The bacterial proteins catalyze the electrogenic symport of glutamate with two protons or a proton and a sodium ion. The eukaryotic glutamate transporters catalyze the electrogenic symport of glutamate with three sodium ions and one proton, whereas one potassium ion is antiported.

The location of the most carboxyl-terminally located membrane-spanning segment (segment 8), which enters the membrane from the extracellular side and runs to the cytoplasmic side, is particularly ill defined. Previous cysteine-scanning mutagenesis studies with two glutamate transporters (human EAAT1 and rat EAAT2) have restricted the membrane-spanning segment to a stretch of about 50 amino acids (10, 11). Hydropathy profile analysis is not very helpful in defining the position of segment 8 more accurately because the region is

* This work was supported by the Ministry of Economic Affairs, the Ministry of Education, Culture, and Science, and the Ministry of Agriculture, Nature Management, and Fishery in the framework of an industrial relevant research program of the Netherlands Association of Biotechnology Centers in The Netherlands. The costs of publication of this article were defrayed in part by the payment of page charges. This article must therefore be hereby marked "*advertisement*" in accordance with 18 U.S.C. Section 1734 solely to indicate this fact.

‡ To whom correspondence should be addressed: Dept. of Microbiology, University of Groningen, Kerklaan 30, 9751 NN Haren, The Netherlands. Tel.: 31-50-363-2155; Fax: 31-50-363-2154; E-mail: j.s.lolkema@biol.rug.nl.

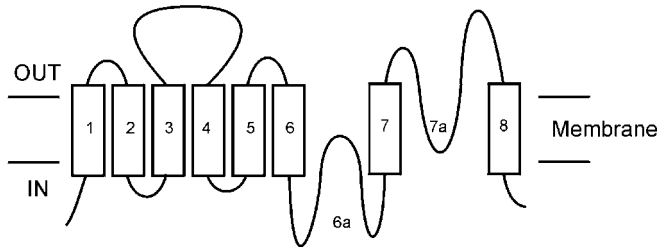

FIG. 1. **Model for the membrane topology of glutamate transporters.** *Numbered rectangles* indicate membrane-spanning segments. The reentrant loops are numbered *6a* and *7a*.

relatively hydrophilic and does not contain a stretch of ~20 hydrophobic residues, which is characteristic for membrane-spanning α-helices. The secondary structure of membrane-spanning segment 8 has been a matter of debate, and it has been modeled both as an α-helix and a β-strand (10, 11, 16, 19). A β-strand structure was suggested because of the hydrophilic nature of the region (11, 19), whereas an α-helical structure was suggested on the basis of computational analysis of periodicity in the amino acid sequences of the glutamate transporters (5, 16). No firm experimental evidence for either structure has been presented.

Here, cysteine-scanning mutagenesis is applied to the region containing membrane-spanning segment 8 in the glutamate transporter GltT of *B. stearothermophilus*. The position of the membrane-spanning segment is confined to a stretch of 23 amino acids, which is likely to adopt an α-helical conformation. The segment lines an aqueous channel and contains many residues that are of crucial importance for glutamate binding and transport.

EXPERIMENTAL PROCEDURES

Bacterial Strains and Growth Conditions

Escherichia coli strain ECOMUT2, which lacks the glutamate transporter GltP (20), was used to express GltT mutants and was grown in Luria Broth medium at 37 °C. Chloramphenicol and ampicillin were used at final concentrations of 30 μg/ml and 100 μg/ml, respectively. Expression of GltT mutants from pBAD24-derived plasmids (21) was induced by adding 0.15% L-arabinose at an A_{600} of 0.5, and cells were harvested 1.5 h after induction.

Recombinant DNA Techniques

General molecular biological techniques are described by Sambrook *et al.* (22). Enzymes for recombinant DNA work were obtained from Roche Molecular Biochemicals (Germany). The polymerase chain reaction overlap extension method (23) was used to introduce mutations in the *gltT* gene on a pBAD24-derived expression plasmid, which encodes GltT with an amino-terminal His tag consisting of six adjacent histidines (9). Oligonucleotides were obtained from Life Technologies, Inc. All polymerase chain reaction-amplified DNA fragments were sequenced by BMTC (Groningen, The Netherlands).

Preparation of Membrane Vesicles

Membrane vesicles with a rightside-out orientation were prepared from *E. coli* ECOMUT2 cells expressing GltT mutants by the osmotic lysis procedure, as described by Kaback (24). Randomly oriented membrane vesicles and membrane vesicles with an inside-out orientation were prepared with sonication and passage through a French pressure cell, respectively, as described previously (9). Membrane vesicles were stored in liquid nitrogen at a protein concentration of 10 mg/ml in 50 mM potassium phosphate, pH 7. The protein concentration was determined with the DC protein assay from Bio-Rad. Expression levels of His-tagged proteins were determined by running membrane vesicles (20 μg of protein) on SDS-polyacrylamide gels followed by transfer to poly(vinylidene difluoride) membranes (Roche Molecular Biochemicals) and detection with monoclonal antibodies directed against a 6 His tag (Dianova, Hamburg, Germany). Antibodies were visualized by using the Western light chemiluminescence detection kit (Tropix, Bedford, MA).

Purification and Reconstitution

GltT mutant proteins were purified and reconstituted into proteoliposomes as described before (25) with the following minor modifications. The detergent *n*-dodecyl-β-D-maltoside (Anatrace, Ohio) was used instead of Triton X-100 to solubilize cytoplasmic membranes (0.4 mg/4 mg of membrane protein) and during purification of GltT (0.03%). Triton X-100 was still used to destabilize preformed liposomes (25). The lipid to protein ratio during reconstitution was 330 (w/w). The protein concentration was determined with the DC protein assay from Bio-Rad. Proteoliposomes were stored in liquid nitrogen an appropriate buffer (see below).

Labeling of Membrane Vesicles and Proteoliposomes

Unless stated otherwise, membrane vesicles with a rightside-out orientation (10 mg of protein/ml) were labeled for 10 min at room temperature with 0.25 mM *N*-ethylmaleimide (NEM)[1] or with the methanethiosulfonate reagents (2-(trimethylammonium)ethyl) methanethiosulfonate bromide (MTSET, 1 mM) and 2-aminoethyl methanethiosulfonate hydrobromide (MTSEA, 2.5 mM) (Anatrace, Ohio). Immediately after labeling, glutamate uptake experiments were performed with these membrane vesicles using artificial gradients.

Membrane vesicles with a random orientation (500 μl, 2 mg of protein/ml in 50 mM potassium phosphate, pH 7) were labeled with 0.25 mM fluorescein maleimide (Molecular Probes, Eugene, Oregon) for 10 min at room temperature. The reaction was stopped by adding a 10-fold excess of dithiothreitol, followed by small scale purification of His-tagged GltT mutants using Ni^{2+}-nitrilotriacetic acid agarose (9). Purified proteins were run on SDS-polyacrylamide gels. Fluorescence of proteins labeled with fluorescein maleimide was visualized by UV excitation using a Gel-Doc system (Bio-Rad).

Proteoliposomes (30 μg of protein) were labeled with 0.25 mM NEM or 0.25 mM 4-acetamido-4′-maleimidylstilbene-2,2′-disulfonic acid (AMdiS) at room temperature for 10 min in 50 mM potassium phosphate, pH 7. The reaction was stopped with a 10-fold excess of dithiothreitol. The labeled proteoliposomes were washed once with 50 mM potassium phosphate, pH 7, and solubilized in 300 μl of the same buffer containing 2% Triton X-100. 0.25 mM fluorescein maleimide was added, and the mixture was incubated for 10 min at room temperature. The reaction was stopped with a 10-fold excess of dithiothreitol. Proteins were precipitated with trichloroacetic acid and run on SDS-polyacrylamide gels. Fluorescence of proteins labeled with fluorescein maleimide was visualized using a Lumi-imager (Roche).

Glutamate Transport Assays

Membrane Vesicles—Glutamate uptake in rightside-out membrane vesicles was measured by rapid filtration. Membrane vesicles were either energized using the potassium ascorbate/phenazine methosulfate electron donor system or by artificial gradients. In the former case, the membranes were diluted to a concentration of 0.6 mg/ml in 50 mM potassium phosphate, pH 7, and 10 mM potassium ascorbate. The uptake experiments were performed in 100 μl at 30 °C under a constant flow of water-saturated air. Phenazine methosulfate was added at a concentration of 100 μM, and the proton motive force was allowed to develop for 2 min, after which L-[^{14}C]glutamate (Amersham Pharmacia Biotech) was added to a final concentration of 1.9 μM. The uptake was stopped by adding a 20-fold excess of ice-cold 0.1 M LiCl solution, followed by immediate filtration over cellulose nitrate filters (pore size, 0.45 μm). The filters were washed once with 2 ml of 0.1 M LiCl and assayed for radioactivity. When artificial gradients were used, a buffer system described previously was used (20). Membrane vesicles (10 mg protein/ml) were loaded with a buffer containing 25 mM potassium phosphate, pH 7, 100 mM potassium acetate, pH 7, and 1 μM valinomycin. Proton motive force-driven uptake was initiated by diluting the 4-μl vesicles into 330 μl of buffer containing 125 mM MES, adjusted to pH 6 with methylglucamine, 1 μM valinomycin, and 0.6 μM L-[^{14}C]glutamate and incubated at 30 °C. The uptake was stopped as described above.

Proteoliposomes—For counterflow experiments proteoliposomes were loaded with 25 mM potassium phosphate and 5 mM potassium glutamate, pH 7, by freeze thawing followed by extrusion through polycarbonate filters (pore size, 400 nm). Proteoliposomes were concentrated by centrifugation (250,000 × *g*, 20 min, 10 °C) and resuspended

[1] The abbreviations used are: NEM, *N*-ethylmaleimide; MTSET, (2-(trimethylammonium)ethyl) methanethiosulfonate bromide; MTSEA, 2-aminoethyl methanethiosulfonate hydrobromide; AMdiS, 4-acetamido-4′-maleimidylstilbene-2,2′-disulfonic acid; MES, 2-(*N*-morpholino)ethanesulfonic acid..

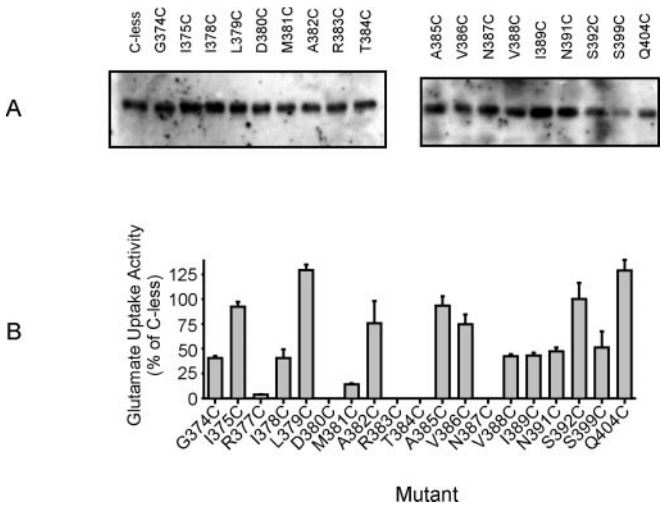

FIG. 2. **Activity and expression of single cysteine GltT mutants.** *Panel A*, expression levels of the mutants on Western blots stained with antibodies raised against the His tag. Mutant R377C is not shown, but see Figs. 3*B* and 7*A*. *Panel B*, initial rates of glutamate uptake in rightside-out membrane vesicles containing the single cysteine mutants were expressed as a percentage of the rate in membrane vesicles containing the cysteineless mutant.

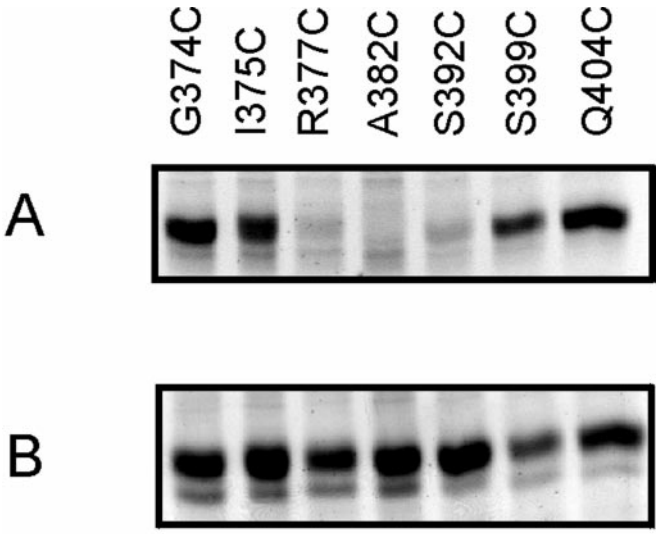

FIG. 3. **Fluorescein maleimide labeling of single cysteine mutants.** Membrane vesicles from cells expressing single cysteine mutants were labeled with fluorescein maleimide, and His-tagged proteins were purified and run on SDS-polyacrylamide gels. *Panel A*, fluorescence of fluorescein maleimide-labeled proteins in the gel using UV excitation. *Panel B*, the same gel was stained with Coomassie Brilliant Blue to compare the amounts of protein.

at a protein concentration of ~0.2 mg/ml. Counterflow was initiated by diluting 4 μl of proteoliposomes into 330 μl of 30 mM potassium phosphate, pH 7, prewarmed at 30 °C, and containing 1.2 μM L-[^{14}C]glutamate. The uptake was stopped as described above. Glutamate uptake driven by artificial gradients in proteoliposomes was assayed using the same procedure as described for counterflow but with the buffer system for artificial gradient described above.

To measure efflux, proteoliposomes were loaded with L-[^{14}C]glutamate using the artificial gradient method until ~10 pmol/μg of protein was taken up by the proteoliposomes. 10 μM Carbonyl cyanide *p*-trifluoromethoxyphenylhydrazone was added, and the efflux reaction was stopped at several time points by diluting aliquots of the reaction mixture in ice-cold 0.1 M LiCl followed by rapid filtration as described above.

RESULTS

Construction, Expression, and Activity of Single Cysteine Mutants—The cysteineless version of GltT, which was shown previously to have glutamate uptake activity similar to that of the wild type (9), was used as background for the construction of a set of 21 single cysteine mutants in the region of membrane-spanning segment 8 (Fig. 1). Each residue in the amino acid stretch that is highly amphipathic when modeled an α-helix (residues 374–392) (5) was mutated to cysteine, as well as selected residues at the carboxyl-terminal end of the stretch. Out of the 21 mutants 19 could be expressed in *E. coli* and were present in the cytoplasmic membrane as judged from Western blots using antibodies raised against the amino-terminal His tag which is present in all mutants (Fig. 2*A*). Only two mutants, D376C and G390C, were not found in the membrane of *E. coli* (not shown). The glutamate transport activity of the mutants that were expressed was measured in membrane vesicles with a rightside-out orientation. At most of the positions cysteine mutations were well tolerated by the transporter resulting in glutamate transport activities between 40 and 125% of the cysteineless mutant (Fig. 2*B*). In four mutants (D380C, R383C, T384C, and N387C) glutamate transport was completely abolished. In two other mutants, R377C and M381C, glutamate uptake was measurable but severely impaired (5 and 17% of the activity of the cysteineless mutant, respectively) (Fig. 2*B*). In none of these mutants was the impaired or abolished activity caused by a reduced level of expression (Fig. 2*A*).

Labeling of Single Cysteine Mutants with Fluorescein Maleimide—The accessibility of the cysteine residues in the GltT mutants for the large maleimide compound fluorescein maleimide (molecular weight 427) was determined. Randomly oriented membrane vesicles were prepared from cells expressing the various GltT mutants and labeled with fluorescein maleimide. Subsequently, the vesicles were solubilized, and His-tagged GltT mutants were purified, followed by SDS-polyacrylamide gel electrophoresis. Fluorescence of GltT mutants labeled with fluorescein maleimide was detected by UV excitation.

The cysteineless mutant was used as a negative control and was not modified by fluorescein maleimide (not shown). Only four single cysteine mutants (G374C, I375C, S399C, and Q404C) were labeled with fluorescein maleimide (Fig. 3). The cysteine residues in the four mutants are located at the extreme amino and carboxyl termini of the mutated stretch. The accessibility of these residues for fluorescein maleimide indicates a location in the protein structure, which is well exposed to the aqueous environment and is consistent with a position in a loop structure. The other single cysteine mutants could not be labeled with fluorescein maleimide, as exemplified by mutants R377C, A382C, and S392C (Fig. 3). The cysteine residues in these mutants are either buried in the protein structure or exposed to the lipid environment.

Although mutants G374C, I375C, and S399C were readily labeled with fluorescein maleimide, the accessibility of the cysteine residues in these mutants is not completely unrestricted: biotin maleimide (molecular weight 524), which was used previously in membrane topology studies of GltT (9), did not label these mutants (not shown). Only the single cysteine in mutant Q404C was readily labeled with biotin maleimide in membrane vesicles with an inside-out orientation, and labeling was prevented by preincubation with the charged maleimide AMdiS, suggesting a cytoplasmic location (9). In agreement, Q404C was not labeled with biotin maleimide in whole cells (not shown).

Effect of NEM, MTSEA, and MTSET on Transport Activity—The effect of cysteine modification on glutamate transport activity was determined in membrane vesicles with a rightside-out orientation prepared from *E. coli* cells expressing the single cysteine mutants. Three small modifying reagents were used:

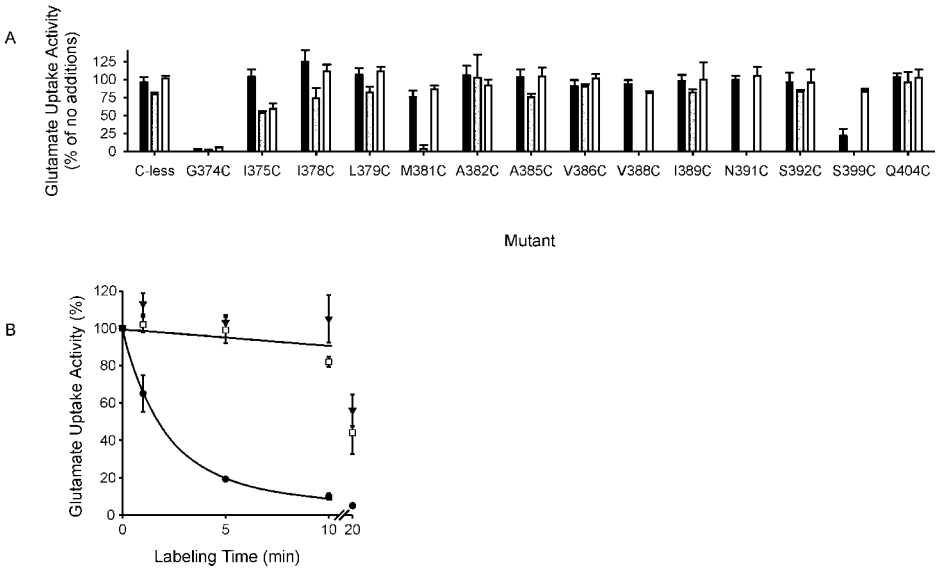

FIG. 4. **Effect of treatment of GltT single cysteine mutants with cysteine-modifying reagents.** *Panel A*, initial rates of glutamate uptake in rightside-out membrane vesicles after treatment with NEM (*black bars*), MTSEA (*gray bars*), and MTSET (*white bars*). Rates were expressed as percentage of the initial rates in untreated membrane vesicles. *Panel B*, kinetics of inactivation of GltT mutants with MTSET. Membrane vesicles with a rightside-out orientation expressing mutants G374C (λ), V388C (θ), and N391C (τ) were treated with MTSET for the indicated time periods, immediately followed by glutamate uptake assays. Initial rates of proton motive force-driven glutamate uptake were expressed as a percentage of the rates in untreated membrane vesicles. G374C, *closed circles*; V388C, *open squares*; and N391C, *closed triangles*.

NEM and MTSEA, which are membrane-permeable, and MTSET, which is charged and reportedly membrane-impermeable (26, 27). Treatment with NEM did not affect glutamate uptake of the cysteineless mutant when the vesicles were energized with the artificial electron donor system ascorbate/phenazine methosulfate (9). In contrast, the methanethiosulfonate reagents severely reduced glutamate uptake activity by the cysteineless mutant using the same energizing method. Apparently, the reagents interfere with the generation of a proton motive force by inhibition of one of the components of the electron transport chain. Therefore, the proton motive force was generated using a combination of acetic acid and K^+ diffusion gradients (20). Glutamate transport catalyzed by the cysteineless mutant driven by the diffusion gradients was not significantly affected by the methanethiosulfonate reagents or NEM (Fig. 4*A*).

One of the four mutants that were labeled with fluorescein maleimide (Fig. 3), G374C, was inactivated by both the membrane-permeable and membrane-impermeable modifying reagents, consistent with accessibility from the outside (Fig. 4*A*). In contrast, mutant S399C was inactivated by the membrane-permeable reagents MTSEA and NEM but not by the membrane-impermeable MTSET. This behavior is consistent with a cytoplasmic accessibility. The other mutants that were labeled with fluorescein maleimide, I375C and Q404C, were not inactivated by NEM (Fig. 4*A*). Similarly the MTS reagents did not inactivate mutant Q404C, whereas the activity of mutant I375C was only slightly affected by the reagents. Apparently, modification of the single cysteines in these mutants is well tolerated.

In the set of single cysteine mutants that were not labeled with fluorescein maleimide, three mutants, M381C, V388C, and N391C, could be inactivated by the membrane-permeable reagent MTSEA but not by the membrane-impermeable reagent MTSET and also not by NEM (Fig. 4*A*). Apparently, accessibility of the cysteine residues is very much restricted, allowing the small and flexible MTSEA reagent, but not NEM, which has a more constrained structure, to reach the residues. Because the membrane-impermeable analogue MTSET did not inhibit the three mutants, the cysteines in the mutants appear to be accessible through a narrow aqueous pore from the cytoplasmic side of the membrane.

Finally, the activity of most of the mutants that were not labeled with fluorescein maleimide was not affected by any of the modifying reagents. These mutants either tolerated modification or could not be modified at all because they were not accessible. Based on the results described here it is not possible to distinguish between the two possibilities. When the region between Gly-374 and Ser-392 is modeled as an α-helix, all inactive, severely impaired, and nonexpressed mutants cluster on one face of the helix (*black circles* in Fig. 5*B*), whereas the active mutants cluster on the other face (*bars* in Fig. 5*A* and *open circles* in 5*B*). The mutants that were inactivated by the cysteine-modifying reagents also cluster on one face of the helix. This face partially overlaps with the face of the helix containing the inactive mutants (*gray bars* and *gray circles* in Fig. 5, *A* and *B*, respectively).

Kinetics of MTSET Labeling—Mutant G374C that is accessible from the periplasmic side of the membrane was inactivated with the membrane-impermeable reagent MTSET with a half-time of 1–2 min (Fig. 4*B*). Mutant S399C that is located at the cytoplasmic side of the membrane was not significantly inactivated in 10 min. However, longer incubations did result in partial inactivation of the mutant. This is most likely caused by a slow permeability of the reagent followed by access from the cytoplasmic side of the membrane. Similar observations were made for mutants M381C, V388C, and N391C (shown for V388C and N391C in Fig. 4*B*), suggesting a similar accessibility from the cytoplasmic side of the membrane following the slow permeation of the reagent.

Orientation of GltT in Proteoliposomes—A more detailed kinetic characterization of the single cysteine mutants was done in proteoliposomes. A procedure to purify GltT and to reconstitute the protein into proteoliposomes was described before (25). To interpret correctly results obtained with single cysteine mutants reconstituted in proteoliposomes (below), the orientation of GltT in the liposomal membrane was determined. Two single cysteine mutants, S129C and S292C, which were characterized before and which contain cysteines with well defined extra- and intracellular locations, respectively (9), were purified and reconstituted into proteoliposomes. The membrane-impermeable maleimide AMdiS was used to label cysteines that are accessible from the outside of the proteoliposomes, whereas NEM was used to label cysteines on both sides of the membrane. Subsequently, unreacted cysteines were labeled with fluorescein maleimide, and the extent of fluorescein labeling was measured. In proteoliposomes, mutant S129C, which has an extracellular cysteine, was fully accessible for both AMdiS and NEM, indicating that the orientation of the protein in the proteoliposomes is rightside-out (Fig. 6). Consistent with

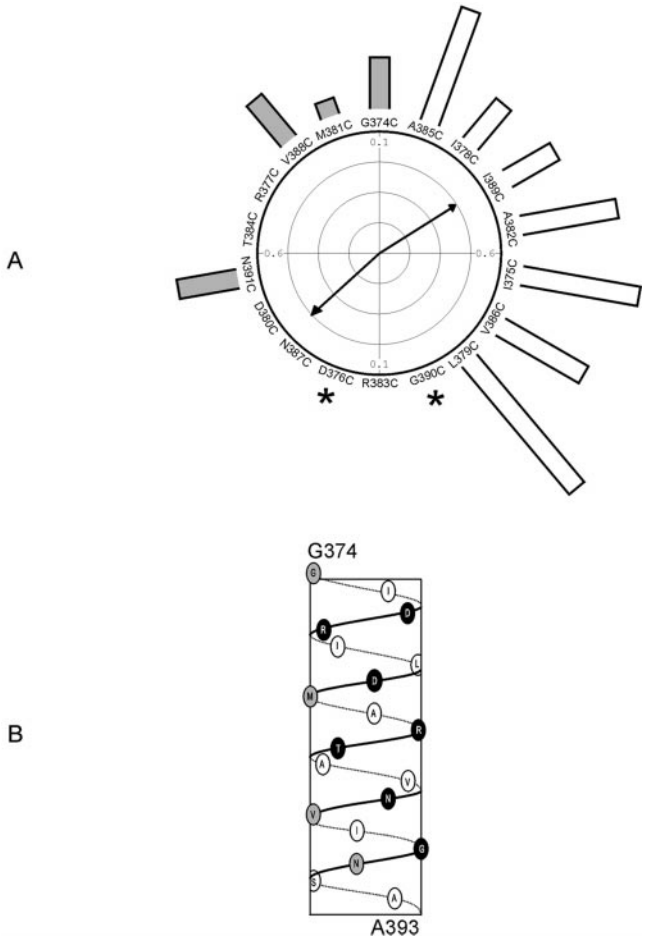

FIG. 5. **α-Helical model of the stretch between Gly-374 and Ser-392.** *Panel A*, helical wheel representation of the amino acid sequence between Gly-374 and Ser-392 modeled as an α-helix. The *bars* represent the activities of the single cysteine mutants at each position. *Shaded bars* indicate activities that were blocked by cysteine-modifying reagents (Fig. 4*A*). *Asterisks* indicate mutants that were not expressed. The *arrows* pointing to the *right* and *left* represent the hydrophobic and substitution moments, respectively, as calculated previously (16). *Panel B*, side view of the α-helical model of the region between Gly-374 and Ser-392. *Solid* and *dashed lines* connect residues on the front and the back of the helix, respectively. The positions of the cysteine residues in mutants that are susceptible for inactivation by cysteine-modifying reagents and the residues of which cysteine mutation results in inactive or nonexpressed mutants are shown in *gray* and *black*, respectively.

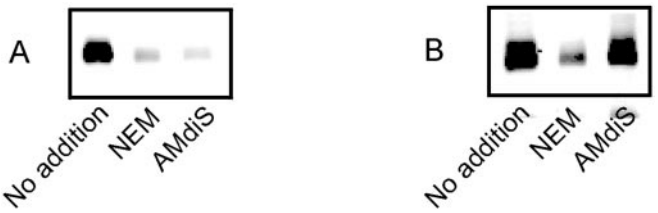

FIG. 6. **Orientation of GltT in proteoliposomes.** Proteoliposomes containing mutants S129C (*panel A*) and S292C (*panel B*) were treated with NEM, AMdiS, or buffer (no addition). Unmodified cysteines were labeled with fluorescein maleimide, and the proteins were run on SDS-polyacrylamide gels. Fluorescence of fluorescein maleimide-labeled proteins in the gel was measured using UV excitation.

this result, the single cysteine in mutant S292C, which has an intracellular location, was accessible for NEM but not for the membrane-impermeable AMdiS. The rightside-out orientation of GltT in proteoliposomes allows a fair comparison of the studies with membrane vesicles and proteoliposomes.

Glutamate Transport Activity in Proteoliposomes—Transporter mutants that do not show activity when transport is

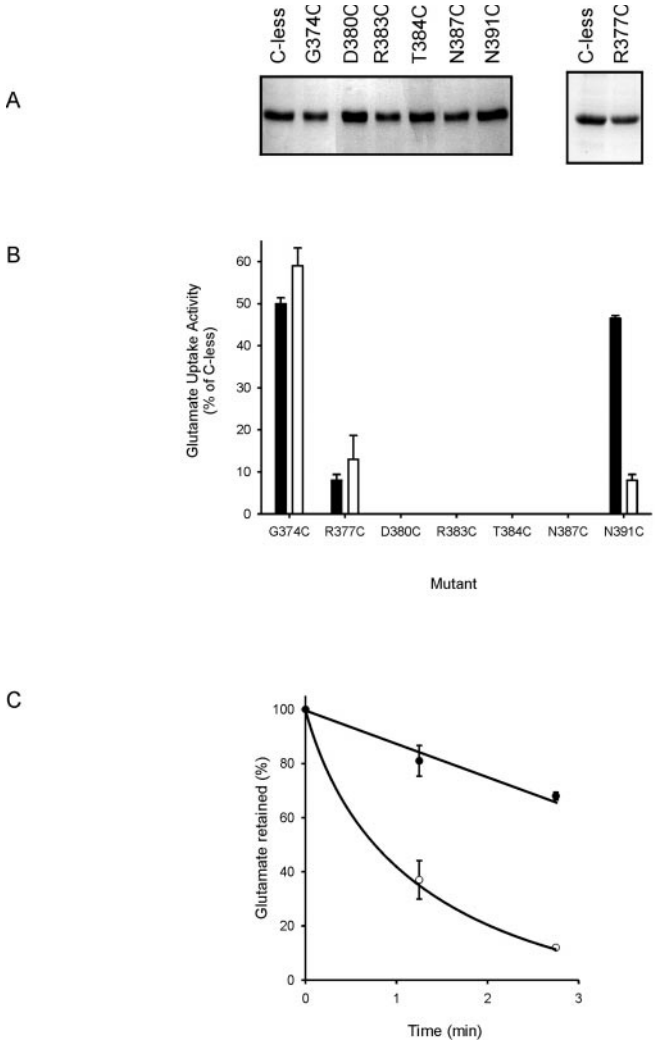

FIG. 7. **Activity of GltT mutants in proteoliposomes.** *Panel A*, Coomassie Brilliant Blue-stained SDS-polyacrylamide gels of GltT mutants purified on Ni^{2+}-NTA agarose columns. *Panel B*, initial rates of proton motive force- and counterflow-driven glutamate uptake in proteoliposomes (*black* and *white bars*, respectively). Rates are expressed as percentage of the initial rate of glutamate uptake in proteoliposomes containing the cysteineless mutant. *Panel C*, efflux of radiolabeled glutamate from proteoliposomes containing the cysteineless mutant (○ or mutant N391C (●).

driven by the proton motive force may show activity when assayed for a partial transport reaction like exchange (see, e.g. Refs. 13 and 28). In such cases the mutant transporter may be unable to complete the catalytic cycle because the reorientation of the unloaded carrier is impaired, a step that is omitted in the exchange mode, whereas the reorientation of the substrate-loaded carrier is unaffected. The exchange reaction catalyzed by GltT was measured using a previously described counterflow assay in proteoliposomes (25). Mutants R377C, D380C, R383C, T384C, and N387C, which were inactive or showed severely impaired glutamate transport activity (Fig. 2), as well as the cysteineless mutant and mutants G374C and N391C, were successfully purified and reconstituted into proteoliposomes using the protocol developed for the wild-type protein (Fig. 7*A*). Proton motive force-driven glutamate uptake of the mutant proteins in proteoliposomes was comparable with the activity in membrane vesicles (Fig. 7*B*, *solid bars*). G374C and N391C showed approximately 50% of the activity of the cysteineless mutant, transport by R377C was severely impaired, but measurable and the other transporters were inactive.

When counterflow was measured the results did not differ

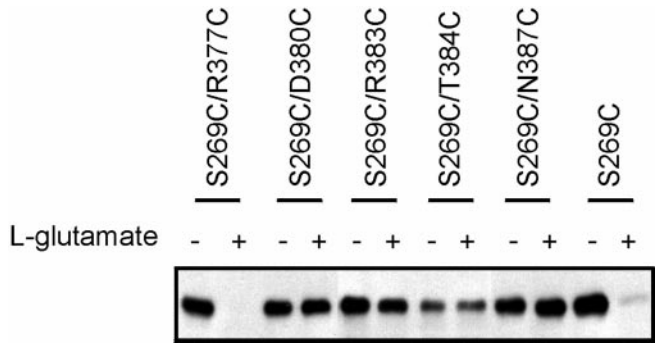

FIG. 8. **Protection by L-glutamate against labeling of Cys-269 with biotin maleimide in double mutants of GltT.** Western blots are shown of purified mutant S269C and double mutants S269C/R377C, S269C/D380C, S269C/R383C, S269C/T384C, and S269C/N287C labeled with biotin maleimide in whole cells in the presence (+) or absence (−) of 5 mM L-glutamate. Western blots were decorated with streptavidin coupled to alkaline phosphatase to detect biotinylated proteins.

significantly from proton motive force-driven transport for most mutants (Fig. 7*B*, *open bars*), indicating that mutants R377C, D380C, R383C, T384C, and N387C are not only impaired in the complete reaction cycle but also in the partial exchange reaction. Surprisingly, counterflow by mutant N391C was severely reduced compared with proton motive force-driven transport. Because efflux catalyzed by mutant N391C is also severely reduced (Fig. 7*C*), the impaired counterflow activity of the mutant was not caused an inability to maintain the necessary gradient of glutamate across the membrane. Therefore, the reduced counterflow activity of mutant N291C may be the result of a reduced affinity for cytoplasmic glutamate, an impaired reorientation of the substrate loaded carrier, or a stringent dependence on the presence of the proton motive force even in the exchange mode.

Glutamate Binding—A qualitative method was developed to measure glutamate binding in GltT mutants R377C, D380C, R383C, T384C, and N387C, which were inactive or severely impaired in proton motive force-driven glutamate uptake. The previously described single cysteine mutant S269C in the reentrant loop between membrane-spanning helix 6 and 7 (Fig. 1) could be labeled with biotin maleimide in whole cells, and labeling was prevented by the presence of L-glutamate (Fig. 8) (9). In contrast, none of the inactive mutants described here (R377C, D380C, R383C, T384C, and N387C) could be labeled with biotin maleimide, either in whole cells or in membrane vesicles (not shown). Double mutants were constructed in which mutation S269C was combined with each of the five mutations that impaired glutamate transport. The double mutants were expressed in *E. coli* and could be labeled in whole cells with biotin maleimide, just like the single mutant S269C (Fig. 8). In the double mutants the cysteine at position 269 serves as indicator for glutamate binding. Labeling of the cysteine in double mutant R377C/S269C could be prevented by the presence of glutamate, indicating normal glutamate binding, even though mutant R377C displayed strongly reduced glutamate transport activity (Figs. 2 and 7). 5 mM L-glutamate did not prevent the labeling with biotin maleimide of the double mutants D380C/S269C, R383C/S269C, T384C/S269C, and N387C/S269C, indicating that in these mutants glutamate binding is completely abolished.

DISCUSSION

Cysteine-scanning mutagenesis has been used to study the membrane topology of several members of the family of glutamate transporters (7–11). The proteins have a highly unusual structure, consisting of eight membrane-spanning segments and two reentrant loops (Fig. 1). There is still some controversy about the exact membrane topology of part of the proteins and, in particular, on the exact position and secondary structure of the most carboxyl-terminal, inward-going, membrane-spanning segment (segment 8). In this report, membrane-spanning segment 8 was studied by cysteine-scanning mutagenesis in the glutamate transporter GltT of the bacterium *B. stearothermophilus*. 21 single cysteine mutants were constructed in a stretch of 30 residues from Gly-374 to E-404, and the membrane-spanning segment could be confined to this stretch by the following criteria.

One mutant (G374C) reacted with both charged and uncharged cysteine-modifying reagents in membrane vesicles with a rightside-out orientation, consistent with a location in an aqueous environment at the extracellular side of the membrane. Furthermore, the bulky molecule fluorescein maleimide labeled the cysteine as well as the cysteine at the adjacent position in mutant I375C, indicative of a spacious access route and a location in a loop structure outside of the membrane. The result is consistent with cysteine-scanning mutagenesis studies in the human glutamate transporter EAAT1, where a cysteine at the corresponding position (A470C) was modeled at the extracellular side of the membrane (11).

In contrast, mutant S399C, the more carboxyl-terminal mutant Q404C, and the previously described mutant Q412C had labeling characteristics of residues located in a loop structure in the aqueous environment at the cytoplasmic side of the membrane. The cysteines in these mutants were accessible for the bulky molecule fluorescein maleimide. Furthermore, mutant S399C was labeled with membrane permeable cysteine-modifying reagents only in membrane vesicles with a rightside-out orientation. Cysteines at positions between Ile-375 and Ser-399 were not labeled with fluorescein maleimide. Therefore, the location of the eighth membrane-spanning segment seems to be confined to a stretch of 23 residues between Ile-375 and Ser-399, which is significantly shorter compared with previous studies that showed at least 50 residues between residues at the extra- and intracellular side of the membrane (10, 11).

The secondary structure of membrane-spanning segment 8 has been a matter of debate, and it has been modeled as both as an α-helix and a β-strand (10, 11, 16, 19). Because a hydrophobic stretch of approximately 20 residues, which is indicative of a membrane-spanning α-helix, is not found at the position of segment 8, the presence of a membrane-spanning β-strand was suggested (11, 19). On the other hand, the stretch of amino acid residues that we experimentally showed to be membrane-spanning has been modeled as an α-helix before, based on computational analysis of the periodicity in the amino acid sequences of glutamate transporters (5, 16). When modeled as an α-helix the region between Gly-374 and Ser-392 is highly amphipathic (Fig. 5*A*) with all well conserved charged and polar residues clustering on one face of the helix and all hydrophobic residues, which are not conserved, clustering on the opposite face (16). Periodicity consistent with an α-helical conformation is also observed in the properties of the cysteine mutants described here. All positions at which cysteine mutations are tolerated cluster on the hydrophobic, nonconserved face of the helix, whereas residues that cannot be mutated to cysteine without loss of activity cluster on the opposite face of the helix (Fig. 5, *A* and *B*). Furthermore, cysteine mutants that can be inactivated by cysteine-modifying reagents also cluster on the same face of the helix. The results strongly suggest that membrane-spanning segment 8 is α-helical. An α-helical conformation of the segment would solve the problem of accommodating the charged and polar residues in the hydrophobic core of the membrane. If the hydrophilic face of the helix were buried

within the protein core it would be effectively shielded from the hydrophobic lipid bilayer by the hydrophobic face.

Interestingly, cysteine residues in three mutants (M381C, V388C, and N391C), which are distributed along the long axis of membrane-spanning helix 8 at the hydrophilic face, were accessible for the cysteine-modifying reagent MTSEA (Fig. 4). This indicates that there must be an aqueous path through the protein which provides an access route to the residues. The water-filled pore is not very spacious because only small and flexible cysteine-modifying reagents can enter it. The narrow aqueous path along membrane-spanning helix 8 contrasts with the very spacious water-filled pore, which was found around the reentrant loop between helices 6 and 79. Therefore, it is unlikely that the two water-accessible pores are parts of one single larger pore. Cysteine-scanning mutagenesis in two related glutamate transporters, human EAAT1 and rat EAAT2, showed that helix 7 also contains water-accessible residues of which the accessibility is restricted to small reagents (7, 11, 12). The similar accessibility behavior of helices 7 and 8 suggests that the two helices may be close together in space.

Since the first mutagenesis experiments of glutamate transporters it is known that certain residues in membrane-spanning helix 8 are of crucial importance for function (11, 28–30). Particularly well characterized is the arginine residue at the corresponding position of Arg-383 in GltT, which is conserved in all glutamate transporters of the family (5). Mutations at this position in the human glutamate transporters EAAT1 and EAAT3 as well as the glutamate transporters EAAT1 and EAAT2 from rat completely abolished glutamate transport (11, 28–30). Interestingly, the arginine mutant in EAAT3 (R447C) was still able to transport cysteine, which is a substrate of EAAT3 but not of the other glutamate transporters. It was concluded that Arg-447 is involved in the binding of the γ-carboxylate group of glutamate (28). The observation that mutant R383C in GltT was completely inactive and could not bind glutamate is consistent with the findings in EAAT3.

In addition, the results presented here show that many other residues at the hydrophilic face of membrane-spanning helix 8 at positions ranging from the extracellular to the cytoplasmic side of the membrane are of crucial importance for the transporter's function. Starting at the amino-terminal end of the helix, mutant R377C was severely impaired in glutamate transport but could still bind glutamate. Subsequently, three mutants, D380C, T384C, and N387C, behaved similarly to mutant R383C: These mutants do not transport glutamate in either the proton motive force-driven uptake mode or the exchange mode and do not bind glutamate. Finally, three mutants, M381C, V388C, and N391C, with cysteines at the hydrophilic face of the helix, could be inactivated by cysteine-modifying reagents. In the latter mutant glutamate exchange and efflux activities were severely impaired, whereas proton motive force-driven glutamate uptake was only mildly affected. Possibly, Asn-391 is involved in binding of cytoplasmic glutamate, which would be consistent with its location at the cytoplasmic end of membrane-spanning segment 8.

In addition to membrane-spanning segment 8 several other regions in the glutamate transporters are important for binding of glutamate, binding of cotransported cations, and translocation. These regions include the reentrant loop between helices 6 and 78, 9, helix 77, 13, 15, and the reentrant loop between helices 7 and 814. Further work is required to find the spatial relation between these regions. In such studies the multimeric structure of the transporters will also have to be considered. Recently, it was reported that the human glutamate transporter EAAT3 is present as a pentamer in oocyte membranes (31). It is not known whether a pentameric structure is common among glutamate transporters and, importantly, whether the monomer subunits functionally interact. Such information will be required to build a model for the substrate binding site and the translocation path.

REFERENCES

1. Otis, T. S., Kavanaugh, M. P., and Jahr, C. E. (1997) *Science* **277,** 1515–1518
2. Nicholls, D., and Attwell, D. (1990) *Trends Pharmacol. Sci.* **11,** 462–468
3. Tanaka, K., Watase, K., Manabe, T., Yamada, K., Watanabe, M., Takahashi, K., Iwama, H., Nishikawa, T., Ichihara, N., Kikuchi, T., Okuyama, S., Kawashima, N., Hori, S., Takimoto, M., and Wada, K. (1997) *Science* **276,** 1699–1702
4. Mennerick, S., and Zorumski, C. F. (1994) *Nature* **368,** 59–62
5. Slotboom, D. J., Konings, W. N., and Lolkema, J. S. (1999) *Microbiol. Mol. Biol. Rev.* **63,** 293–307
6. Lolkema, J. S., and Slotboom, D. J. (1998) *Mol. Membr. Biol.* **15,** 33–42
7. Seal, R. P., and Amara, S. G. (1998) *Neuron* **21,** 1487–1498
8. Grunewald, M., and Kanner, B. I. (2000) *J. Biol. Chem.* **275,** 9684–9689
9. Slotboom, D. J., Sobczak, I., Konings, W. N., and Lolkema, J. S. (1999) *Proc. Natl. Acad. Sci. U. S. A.* **96,** 14282–14287
10. Grunewald, M., Bendahan, A., and Kanner, B. I. (1998) *Neuron* **21,** 623–632
11. Seal, R. P., Leighton, B. H., and Amara, S. G. (2000) *Neuron* **25,** 695–706
12. Zarbiv, R., Grunewald, M., Kavanaugh, M. P., and Kanner, B. I. (1998) *J. Biol. Chem.* **273,** 14231–14237
13. Zhang, Y., Bendahan, A., Zarbiv, R., Kavanaugh, M. P., and Kanner, B. I. (1998) *Proc. Natl. Acad. Sci. U. S. A.* **95,** 751–755
14. Zhang, Y., and Kanner, B. I. (1999) *Proc. Natl. Acad. Sci. U. S. A.* **96,** 1710–1715
15. Kavanaugh, M. P., Bendahan, A., Zerangue, N., Zhang, Y., and Kanner, B. I. (1997) *J. Biol. Chem.* **272,** 1703–1708
16. Slotboom, D. J., Lolkema, J. S., and Konings, W. N. (1996) *J. Biol. Chem.* **271,** 31317–31321
17. Mitrovic, A. D., Amara, S. G., Johnston, G. A., and Vandenberg, R. J. (1998) *J. Biol. Chem.* **273,** 14698–14706
18. Vandenberg, R. J., Arriza, J. L., Amara, S. G., and Kavanaugh, M. P. (1995) *J. Biol. Chem.* **270,** 17668–17671
19. Wahle, S., and Stoffel, W. (1996) *J. Cell Biol.* **135,** 1867–1877
20. Tolner, B., Ubbink-Kok, T., Poolman, B., and Konings, W. N. (1995) *Mol. Microbiol.* **18,** 123–133
21. Guzman, L. M., Belin, D., Carson, M. J., and Beckwith, J. (1995) *J. Bacteriol.* **177,** 4121–4130
22. Sambrook, J., Fritsch, E. F., and Maniatis, T. (1989) *Molecular Cloning: A Laboratory Manual*, 2nd Ed., Cold Spring Harbor Laboratory, Cold Spring Harbor, NY
23. Higuchi, R., Krummel, B., and Saiki, R. K. (1988) *Nucleic Acids Res.* **16,** 7351–7367
24. Kaback, H. R. (1971) *Methods Enzymol.* **22,** 99–120
25. Gaillard, I., Slotboom, D. J., Knol, J., Lolkema, J. S., and Konings, W. N. (1996) *Biochemistry* **35,** 6150–6156
26. Karlin, A., and Akabas, M. H. (1998) *Methods Enzymol.* **293,** 123–145
27. Akabas, M. H., Stauffer, D. A., Xu, M., and Karlin, A. (1992) *Science* **258,** 307–310
28. Bendahan, A., Armon, A., Madani, N., Kavanaugh, M. P., and Kanner, B. I. (2000) *J. Biol. Chem.* **275,** 37436–37442
29. Conradt, M., and Stoffel, W. (1995) *J. Biol. Chem.* **270,** 25207–25212
30. Pines, G., Zhang, Y., and Kanner, B. I.(1995) *J. Biol. Chem.* **270,** 17093–17097
31. Eskandari, S., Kreman, M., Kavanaugh, M. P., Wright, E. M., and Zampighi, G. A.(2000) *Proc. Natl. Acad. Sci. U. S. A.* **97,** 8641–8646